

Article

Adaptive Fuzzy Fixed-Time Control for Uncertain Nonlinear Systems with Mismatched Disturbances

Rongzheng Luo¹, Lu Zhang¹ and You Li^{2,*}

¹ Institute of Remote Sensing Satellite, China Academy of Space Technology, Beijing 100094, China; lrz_519894574@163.com (R.L.); wonderfulday617@163.com (L.Z.)

² School of Aerospace Science and Technology, Xidian University, Xi'an 710126, China

* Correspondence: liyou@xidian.edu.cn

Abstract: This paper focuses on addressing the adaptive fuzzy fixed-time issue for a class of nonlinear systems with uncertainty functions and mismatched disturbances. Fuzzy logical systems are utilized for identifying unknown functions. Additionally, to tackle challenges posed by mismatched disturbances, disturbance observers are constructed based on the backstepping method. Utilizing the adding one power integrator approach and the fixed-time control method, this paper introduces a fixed-time adaptive fuzzy control algorithm. Notably, this algorithm accommodates the presence of unknown mismatched disturbances and nonlinear functions. The paper establishes, through the application of the Lyapunov stability theory, that the designed adaptive fixed-time fuzzy control algorithm ensures practical fixed-time stability for the resulting closed-loop systems. Finally, the effectiveness of the derived strategy is demonstrated through an illustrative example involving two cases.

Keywords: adaptive backstepping control; disturbance observer; fixed-time control



Citation: Luo, R.; Zhang, L.; Li, Y. Adaptive Fuzzy Fixed-Time Control for Uncertain Nonlinear Systems with Mismatched Disturbances. *Symmetry* **2024**, *16*, 560. <https://doi.org/10.3390/sym16050560>

Academic Editor: Hsien-Chung Wu

Received: 18 February 2024

Revised: 8 March 2024

Accepted: 21 March 2024

Published: 4 May 2024



Copyright: © 2024 by the authors. Licensee MDPI, Basel, Switzerland. This article is an open access article distributed under the terms and conditions of the Creative Commons Attribution (CC BY) license (<https://creativecommons.org/licenses/by/4.0/>).

1. Introduction

Over the past decade, finite-time control and backstepping control have emerged as two prominent research focuses in nonlinear systems. They have found widespread application in diverse practical engineering systems, including robot control systems, spacecraft control systems, unmanned marine vehicles, and multi-unmanned aerial vehicles [1–5]. In contrast to asymptotic control strategies, finite-time control strategies offer several advantages, including enhanced disturbance rejection capabilities, higher control precision, and faster convergence rates [6,7]. On the other hand, the technique of backstepping, introduced in 1991 by Kanellakopoulos, has evolved into a commonly employed method for deriving control laws in systems with nonlinear dynamic models [8–10]. It has been instrumental in the progress of systems exhibiting both multi-input and multi-output characteristics, as well as those featuring single-input and single-output attributes [11,12]. It is crucial to emphasize that all the aforementioned control algorithms do not take into account model uncertainties and disturbances.

In real-world engineering applications, uncertainties and disturbances are prevalent [13]. Specifically, systems like multi-missiles and multi-hydraulic manipulators are prone to mismatched uncertainties. External factors, such as wind, variation in parameters, and environmental forces, directly impact the system's performance, bypassing the actuator input pathway [14–16]. Feedback controllers do not have a direct means to mitigate these influences. In recent developments, significant progress has been made in establishing effective methods to bolster the system's resilience in the face of unknown disturbances and uncertainties. Notable examples include H_∞ , terminal sliding-mode control, and controllers utilizing disturbance observers. Among these methods, a control method based on disturbance observers stands out as a promising approach to strike a balance between the

demands of disturbance rejection capabilities and performance indices. In [17], a disturbance observer-based control approach with terminal sliding-mode control was utilized to alleviate the effects of mismatched disturbances, ensuring the stability of the system. In [18], a new finite-time distributed observer-based containment control algorithm was derived for a category of nonlinear multi-agent systems subject to mismatched disturbances. In [19], an innovative method for active anti-disturbance output consensus was introduced for addressing mismatched disturbances in nonlinear multi-agent systems. Nevertheless, the aforementioned robust control approaches can only assure the asymptotical or finite-time stability of the controlled systems.

It is worth noting that a limitation of finite-time control is its dependence on the initial states for convergence time [20–23]. The applicability of finite-time control is impeded by the necessity to have information about initial states for determining convergent time, a requirement that may not always be met due to uncertainties in the initial conditions in real-world applications [24–26]. Hence, the finite-time controller incorporates the concept of fixed-time stability, ensuring that the convergent time remains unaffected by the initial conditions [27–29]. Up to this point, researchers have derived controllers with fixed-time characteristics for nonlinear systems [30–32]. However, these schemes did not consider disturbances and model uncertainties, significantly limiting the applicability of the derived fixed-time control laws. The presence of entirely unknown nonlinear terms and mismatched disturbances adds complexity to the controller design. Under these circumstances, achieving fixed-time control for nonlinear systems with mismatched disturbances becomes a nontrivial challenge, and existing research results are insufficient to address this challenge. This motivation prompted the investigation presented in this paper.

In summary of the preceding discussions, our investigation centers on deriving a fixed-time controller for a category of uncertain nonlinear systems with mismatched disturbances. A pioneering fuzzy fixed-time control algorithm, incorporating disturbance observers, is presented to guarantee the practical fixed-time stability of the controlled systems. The primary contributions of this paper are emphasized as follows: (1) This paper investigates the fixed-time stability problem for nonlinear systems, seeking the convergence of states in the resulting closed-loop system to a small region around the origin within fixed-time. Importantly, the convergence time in this study is unaffected by the initial conditions. Nonetheless, it is acknowledged that initial conditions may significantly influence the convergence time of finite-time controllers in [20,21,33]. (2) Unlike the fixed-time controllers mentioned in [34–38], our approach takes into account mismatched disturbances. The challenge posed by uncertain functions and mismatched disturbances is concurrently addressed by incorporating fuzzy logical systems, adaptive laws, and disturbance observers. (3) In comparison to some studies on fixed-time control, where the terminal sliding mode was applied to design control schemes [38], this paper proposes a new fixed-time control protocol. Designed for uncertain nonlinear systems, it incorporates the adding one power integrator approach and backstepping technique to prevent non-continuous and singular issues.

The remainder of this article is structured as follows. The problem statement and some preliminaries are presented in Section 2. Section 3 provides a comprehensive overview of the principal outcomes related to designing the fixed-time control protocol. Section 4 includes an illustrative example for clarification, and the paper concludes with Section 5.

Notations: $\mathbb{R}^{p \times q}$ represents the set of $p \times q$ real matrices. $\text{sign}(\cdot)$ represents the sign function. $\text{sig}^b(\cdot) = \text{sign}(\cdot) \cdot |\cdot|^b$. $\|\cdot\|$ refers to the Euclidean norm.

2. Problem Formulation

2.1. Problem Formulation

Considering a category of uncertain nonlinear systems,

$$\begin{aligned}\dot{x}_i &= f_i(\bar{x}_i) + x_{i+1} + d_i, \quad 1 \leq i \leq n-1 \\ \dot{x}_n &= f_n(\bar{x}_n) + u + d_n \\ y &= x_1\end{aligned}\quad (1)$$

where $\bar{x}_n = [x_1, \dots, x_n]^T \in \mathbb{R}^n$ represents the plant state vector, $u \in \mathbb{R}$ represents the control input, $y \in \mathbb{R}$ represents the plant output vector. $f_i(\bar{x}_i)$ represents unknown nonlinear functions, and d_i denotes the mismatched disturbance with $i = 1, \dots, n$.

Control objective: to design a fixed-time adaptive fuzzy control algorithm for Equation (1) with mismatched disturbances, which renders the controlled systems practically fixed-time stable. Moreover, all signals in the evolved systems converge to a small region around the origin within fixed-time.

To facilitate the design of the control strategy, some lemmas are given.

Lemma 1. Based on reference [39], for $z_k \in \mathbb{R}$, $k = 1, \dots, p$ and $s > 1$, one has

$$\left(\sum_{k=1}^p |z_k| \right)^s \leq \frac{1}{n^{1-s}} \sum_{k=1}^p |z_k|^s \quad (2)$$

$$\left(\sum_{k=1}^p |z_k| \right)^{1/s} \leq \sum_{k=1}^p |z_k|^{1/s} \quad (3)$$

Lemma 2. Based on reference [39], for $c > 0$, $k > 0$, and $\xi > 0$, we have

$$|x|^c |z|^k \leq \frac{c\xi}{c+k} |x|^{k+c} + \frac{k\xi^{-c/k}}{c+k} |z|^{c+k} \quad (4)$$

Lemma 3. Based on reference [40], for $a \in \mathbb{R}$, $z \in \mathbb{R}$, and $s \geq 1$, one has

$$|a+z|^s \leq 2^{s-1} |\text{sig}^s(a) + \text{sig}^s(z)| \quad (5)$$

$$|a-z|^s \leq 2^{s-1} |\text{sig}^s(a) - \text{sig}^s(z)| \quad (6)$$

Lemma 4. Based on reference [38], for the nonlinear system,

$$\dot{y} = h(y, t), \quad h(0, t) = 0, \quad y \in \mathbb{R}^n \quad (7)$$

Based on us assume the existence of a Lyapunov function $V(y)$ and some positive constants $\varsigma_1, \varsigma_2, m, n \in \mathbb{R}^+$, $\varsigma_2 k > 1$, $\varsigma_1 k < 1$, and $0 < c < \infty$, such that

$$\dot{V}(y) \leq -(mV(y)^{\varsigma_1} + nV(y)^{\varsigma_2})^k + c, \quad y \in U_o \quad (8)$$

Subsequently, the solution of Equation (7) is practical fixed-time and satisfies

$$\left\{ \lim_{t \rightarrow T} y | V(y) \leq \min \left\{ m^{-\frac{1}{\varsigma_1}} \left(\frac{c}{1-\eta^k} \right)^{\frac{1}{\varsigma_1 k}}, n^{-\frac{1}{\varsigma_2}} \left(\frac{c}{1-\eta^k} \right)^{\frac{1}{\varsigma_2 k}} \right\} \right\} \quad (9)$$

where $0 < \eta < 1$. The settling time is given by

$$T \leq \frac{1}{m^k \eta^k (1 - \varsigma_1 k)} + \frac{1}{n^k \eta^k (\varsigma_2 k - 1)} \quad (10)$$

2.2. Fuzzy Logic Systems

The unknown nonlinear term is approximated using fuzzy logical systems (FLSs) in this article, which can be described as

$$y(x) = \frac{\sum_{i=1}^l \theta_i \prod_{i=1}^n \varphi_{F_i^l}(x_i)}{\sum_{i=1}^l \prod_{i=1}^n \varphi_{F_i^l}(x_i)} \quad (11)$$

where $y \in \mathbb{R}$ and $x = [x_1, \dots, x_n]^T \in \mathbb{R}^n$ denote the input and output vector, respectively. $\varphi_{F_i^l}(x_i)$ is membership function, $i = 1, 2, \dots, l$ and l refers the number of rules, $\theta_i = \max_{y \in \mathbb{R}} \varphi_{G^i}(y)$. Then, fuzzy basis functions can be modeled by

$$\varphi_i(x) = \frac{\prod_{i=1}^n \varphi_{F_i^l}(x_i)}{\sum_{i=1}^l [\prod_{i=1}^n \varphi_{F_i^l}(x_i)]} \quad (12)$$

Denote $\theta^T = [\theta_1, \theta_2, \dots, \theta_l]$ and $\varphi^T(x) = [\varphi_1, \varphi_2, \dots, \varphi_l]$. According to Equation (12), one has $\varphi^T(x)\varphi(x) < 1$. Then, based on Equations (11) and (12), we have

$$y(x) = \theta^T \varphi(x) \quad (13)$$

Furthermore, if $f(x)$ is a continuous function defined on a compact set \mathfrak{A} , there exists the FLSs for an arbitrary $\varepsilon > 0$ satisfying the following inequality

$$\sup_{x \in \mathfrak{A}} |f(x) - \theta^T \varphi(x)| \leq \varepsilon \quad (14)$$

Remark 1. In certain earlier studies on nonlinear systems, constraints were imposed on the nonlinear functions to fulfill specific conditions, like the quadratic and Lipschitz conditions [41,42]. Nevertheless, this paper does not impose any requirements to satisfy these constraints. Therefore, this description is more general. Additionally, practical engineering systems may experience mismatched disturbances, which can adversely affect the properties of the control system and potentially induce system instability. Consequently, it is highly significant to consider mismatched disturbances in the design of controllers for these universal systems.

3. Main Results

In this section, we will derive a fixed-time adaptive control law for nonlinear systems encountering mismatched disturbances and uncertainty functions. This will be achieved through the utilization of the adding one power integrator and the backstepping control approach.

3.1. Fuzzy Adaptive Fixed-Time Controller

To streamline the control protocol development, the coordinate transformations ϑ_1 and ϑ_n are formulated as follows:

$$\begin{aligned} \vartheta_1 &= \text{sig}^{1/\tau_1}(x_1) - \text{sig}^{1/\tau_1}(\sigma_1) \\ \vartheta_i &= \text{sig}^{1/\tau_i}(x_i) - \text{sig}^{1/\tau_i}(\sigma_i), i = 2, \dots, n \end{aligned} \quad (15)$$

where $\tau_1 = 1$, $0 < \tau_{i+1} = \tau_i + b < 1$, $-1 < b < 0$, $\sigma_1 = 0$, $\sigma_i (i = 2, \dots, n)$ represent virtual control schemes to be proposed later.

Step 1: Choose the Lyapunov function as

$$V_1 = \int_{\sigma_1}^{x_1} \text{sig}^{2-\tau_2}(\text{sig}^{1/\tau_1}(s) - \text{sig}^{1/\tau_1}(\sigma_1)) ds + \frac{1}{2} \tilde{\chi}^2 + \frac{1}{2} \tilde{\theta}_1^T \tilde{\theta}_1 + \frac{1}{2} \tilde{\Psi}_1^2 \quad (16)$$

where $\hat{\chi}$, $\hat{\theta}_1$, and $\hat{\Psi}_1$ are estimations of χ^* , θ_1 , and Ψ_1 , respectively. $\tilde{\chi} = \chi^* - \hat{\chi}$, $\tilde{\theta}_1 = \theta_1 - \hat{\theta}_1$, $\tilde{\Psi}_1 = \Psi_1 - \hat{\Psi}_1$, and the definitions of χ^* , θ_1 , and Ψ_1 are to be given at a later stage. Based on (16), we obtain

$$\begin{aligned} \dot{V}_1 = & \text{sig}^{2-\tau_2}(\vartheta_1)(x_2 - \sigma_2) + \text{sig}^{2-\tau_2}(\vartheta_1)(f_1(x_1) + d_1(t)) + \text{sig}^{2-\tau_2}(\vartheta_1)\sigma_2 \\ & - \tilde{\chi}\dot{\chi} - \tilde{\theta}_1^T\dot{\theta}_1 - \tilde{\Psi}_1^T\dot{\Psi}_1 \end{aligned} \quad (17)$$

Based on Lemma 1 to 3, we find

$$\text{sig}^{2-\tau_2}(\vartheta_1)(x_2 - \sigma_2) \leq |\vartheta_1|^{2-\tau_2}|x_2 - \sigma_2| \leq 2|\vartheta_1|^{2-\tau_2}|\vartheta_2|^{\tau_2} \leq |\vartheta_1|^2 + \varsigma|\vartheta_2|^2 \quad (18)$$

where $\varsigma = \tau_2(2 - \tau_2)^{(2-\tau_2)/\tau_2} > 0$ is a constant.

The FLSs serve as an approximator to identify $f_1(x_1)$, such that

$$f_1(x_1) = \theta_1^T \varphi_1 + \epsilon_1 \quad (19)$$

where ϵ_1 is the approximate error with $\bar{\epsilon}_1 \geq |\epsilon_1|$ as its upper bound. Let $\Psi_1 = d_1(t) + \bar{\epsilon}_1$, which denotes compound disturbance.

Then, the virtual control scheme σ_2 and update law of $\hat{\theta}_1$ are defined as

$$\sigma_2 = -\text{sig}^{\tau_2}(\vartheta_1)(\ell\hat{\chi} + 1 + \psi) - \frac{1}{4}\text{sig}^{2-\tau_2}(\vartheta_1) - \hat{\theta}_1^T \varphi_1 - \hat{\Psi}_1 - 2^{3\beta-2}|\vartheta_1|^\eta \text{sig}^{\tau_2-2}(\vartheta_1) \quad (20)$$

$$\dot{\hat{\theta}}_1 = \text{sig}^{2-\tau_2}(\vartheta_1)\varphi_1 - \gamma_1\hat{\theta}_1 \quad (21)$$

where $\beta = \frac{\eta}{2-b} > 1$, $\ell > 0$, $\eta > 2 - b$, $\gamma_1 > 0$, and $\psi > 0$ are parameters.

Construct the disturbance observer as

$$\begin{aligned} \dot{\hat{\Psi}}_1 &= \delta_1(x_1 - \phi_1) \\ \dot{\phi}_1 &= x_2 + \hat{\theta}_1^T \varphi_1 + \hat{\Psi}_1 \end{aligned} \quad (22)$$

where $\delta_1 > 0$ is a design parameter and ϕ_1 denotes an auxiliary function.

Based on Equation (22), we have

$$\dot{\hat{\Psi}}_1 = \delta_1(\tilde{\Psi}_1 + \tilde{\theta}_1^T \varphi_1) \quad (23)$$

Invoking Equations (18) to (23), we have

$$\begin{aligned} \dot{V}_1 \leq & |\vartheta_1|^2 + \varsigma|\vartheta_2|^2 + \text{sig}^{2-\tau_2}(\vartheta_1)(f_1(x_1) + d_1(t)) + \text{sig}^{2-\tau_2}(\vartheta_1)\sigma_2 - \tilde{\chi}\dot{\chi} - \tilde{\theta}_1^T\dot{\theta}_1 - \tilde{\Psi}_1^T\dot{\Psi}_1 \\ \leq & -\psi\vartheta_1^2 - 2^{3\beta-2}|\vartheta_1|^\eta - \vartheta_1^2\ell\hat{\chi} + \varsigma|\vartheta_2|^2 + \text{sig}^{2-\tau_2}(\vartheta_1)(\theta_1^T \varphi_1 + \epsilon_1 + d_1(t) - \hat{\theta}_1^T \varphi_1 \\ & - \hat{\Psi}_1 - \frac{1}{4}\text{sig}^{2-\tau_2}(\vartheta_1)) - \tilde{\chi}\dot{\chi} - \tilde{\theta}_1^T\dot{\theta}_1 - \tilde{\Psi}_1^T\dot{\Psi}_1 \\ \leq & -\psi\vartheta_1^2 - 2^{3\beta-2}|\vartheta_1|^\eta + \text{sig}^{2-\tau_2}(\vartheta_1)(\theta_1^T \varphi_1 + \Psi_1 - \hat{\theta}_1^T \varphi_1 - \hat{\Psi}_1 - \frac{1}{4}\text{sig}^{2-\tau_2}(\vartheta_1)) \\ & - \vartheta_1^2\ell\hat{\chi} + \text{sig}^{1-b}(\vartheta_1)\Omega_1(x) - \tilde{\chi}\dot{\chi} - \tilde{\theta}_1^T\dot{\theta}_1 - \tilde{\Psi}_1^T\dot{\Psi}_1 \end{aligned} \quad (24)$$

Note that $\Omega_1(x) = \text{sig}^{b-1}(\vartheta_1)\varsigma|\vartheta_2|^2$. With the ability of FLSs to approximate $\Omega_1(x_1, \sigma_2)$, one has

$$\Omega_1(x_1, \sigma_2) = \theta_{\Omega_1,1}^T \varphi_{\Omega_1,1} + \epsilon_{\Omega_1} \quad (25)$$

where ϵ_{Ω_1} is the approximation error.

Furthermore, we have

$$\Omega_1 = \theta_{\Omega_1}^T \varphi_{\Omega_1} + \epsilon_{\Omega_1} \leq \bar{\theta}_{\Omega_1}^T \bar{\varphi}_{\Omega_1} \quad (26)$$

where $\bar{\theta}_{\Omega_1}^T = [\theta_{\Omega_1}^T, \bar{\epsilon}_{\Omega_1}]$, $\bar{\epsilon}_{\Omega_1}$ is a positive constant satisfying $\bar{\epsilon}_{\Omega_1} \geq |\epsilon_{\Omega_1}|$, $\bar{\varphi}_{\Omega_1}^T = [\varphi_{\Omega_1}, 1]$. According to Lemma 2 and property $0 < \varphi_{\Omega_1}^T \varphi_{\Omega_1} \leq 1$, we find

$$\text{sig}^{1-b}(\vartheta_1) \Omega_1(x) \leq |\vartheta_1|^{1-b} \bar{h}_1^{\frac{2-\tau_2}{2}} \leq |\vartheta_1|^{1-b} \chi^* \frac{1-b}{2} \leq \ell \vartheta_1^2 \chi^* + \Gamma_1 \quad (27)$$

where $\bar{h}_1 = (\sqrt{2} \|\bar{\theta}_{\Omega_1}\|)^{2/(1-b)}$ and $\Gamma_1 = \frac{1+b}{2} \left(\frac{2}{1-b}\ell\right)^{-(1-b)/(1+b)}$.

Then, substituting Equation (27) into Equation (24) yields

$$\begin{aligned} \dot{V}_1 &\leq -\psi \vartheta_1^2 - 2^{3\beta-2} |\vartheta_1|^\eta - \vartheta_1^2 \ell \hat{\chi} + \ell \vartheta_1^2 \chi^* + \Gamma_1 - \tilde{\chi} \hat{\chi} + \tilde{\Psi}_1 (\Psi_1 - \delta_1 \tilde{\Psi}_1) \\ &\quad + \left(1 + \frac{p}{2} \delta_1^2\right) \tilde{\Psi}^2 + \frac{l}{2p} \|\tilde{\theta}_1\|^2 + \gamma_1 \tilde{\theta}_1^T \hat{\theta}_1 \\ &\leq -\psi \vartheta_1^2 - 2^{3\beta-2} |\vartheta_1|^\eta + \tilde{\chi} (\ell \vartheta_1^2 - \hat{\chi}) + \Gamma_1 + \tilde{\Psi}_1 (\Psi_1 - \delta_1 \tilde{\Psi}_1) \\ &\quad + \left(1 + \frac{p}{2} \delta_1^2\right) \tilde{\Psi}_1^2 + \frac{l}{2p} \|\tilde{\theta}_1\|^2 + \gamma_1 \tilde{\theta}_1^T \hat{\theta}_1 \end{aligned} \quad (28)$$

where p is a design parameter and ι is the node number of FLSs.

Step 2: The Lyapunov function in step 2 is given by

$$V_2 = V_1 + \int_{\sigma_2}^{x_2} \text{sig}^{2-\tau_2+1} (\text{sig}^{1/\tau_2}(s) - \text{sig}^{1/\tau_2}(\sigma_2)) ds + \frac{1}{2} \tilde{\theta}_2^T \tilde{\theta}_2 + \frac{1}{2} \tilde{\Psi}_2^2 \quad (29)$$

Similar to the derivation process in step 1, the virtual control scheme σ_3 and update law of $\hat{\theta}_2$ are defined as

$$\sigma_3 = -\text{sig}^{\tau_3}(\vartheta_2) (\ell \hat{\chi} + 1 + \psi) - \frac{1}{4} \text{sig}^{2-\tau_3}(\vartheta_2) - \hat{\theta}_2^T \varphi_2 - \hat{\Psi}_2 - 2^{3\beta-2} |\vartheta_2|^\eta \text{sig}^{\tau_3-2}(\vartheta_2) \quad (30)$$

$$\dot{\hat{\theta}}_2 = \text{sig}^{2-\tau_3}(\vartheta_2) \varphi_2 - \gamma_2 \hat{\theta}_2 \quad (31)$$

where $\beta = \frac{\eta}{2-b} > 1$, $\ell > 0$, $\eta > 2 - b$, $\gamma_2 > 0$, and $\psi > 0$ are parameters.

Construct the disturbance observer as

$$\begin{aligned} \dot{\hat{\Psi}}_2 &= \delta_2 (x_2 - \phi_2) \\ \dot{\phi}_2 &= x_3 + \hat{\theta}_2^T \varphi_2 + \hat{\Psi}_2 \end{aligned} \quad (32)$$

where $\delta_2 > 0$ is a design parameter and ϕ_2 denotes an auxiliary function.

Then, at step 2, V_2 satisfies

$$\begin{aligned} \dot{V}_2 &\leq -\psi \sum_{k=1}^2 \vartheta_k^2 - 2^{3\beta-2} \sum_{k=1}^2 |\vartheta_k|^\eta + \tilde{\chi} (\ell \sum_{k=1}^2 \vartheta_k^2 - \hat{\chi}) + (2)\Gamma_1 + \sum_{k=1}^2 \tilde{\Psi}_k (\Psi_k - \delta_k \tilde{\Psi}_k) \\ &\quad + \left(1 + \frac{p}{2} \delta_k^2\right) \sum_{k=1}^2 \tilde{\Psi}_k^2 + \frac{l}{2p} \sum_{k=1}^2 \|\tilde{\theta}_k\|^2 + \gamma_k \sum_{k=1}^2 \tilde{\theta}_k^T \hat{\theta}_k \end{aligned} \quad (33)$$

Step i ($3 \leq i \leq n - 1$): The Lyapunov function in step $i - 1$ is given by

$$V_{i-1} = V_1 + \sum_{k=2}^{i-1} \int_{\sigma_k}^{x_k} \text{sig}^{2-\tau_k+1} (\text{sig}^{1/\tau_k}(s) - \text{sig}^{1/\tau_k}(\sigma_k)) ds + \frac{1}{2} \sum_{k=2}^{i-1} \tilde{\theta}_k^T \tilde{\theta}_k + \frac{1}{2} \sum_{k=2}^{i-1} \tilde{\Psi}_k^2 \quad (34)$$

Assume that, at this particular step, V_{i-1} satisfies

$$\begin{aligned} \dot{V}_{i-1} \leq & -\psi \sum_{k=1}^{i-1} \vartheta_k^2 - 2^{3\beta-2} \sum_{k=1}^{i-1} |\vartheta_k|^\eta + \tilde{\chi}(\ell \sum_{k=1}^{i-1} \vartheta_k^2 - \hat{\chi}) + (i-1)\Gamma_1 + \sum_{k=1}^{i-1} \tilde{\Psi}_k(\Psi_k - \delta_k \tilde{\Psi}_k) \\ & + (1 + \frac{p}{2} \delta_k^2) \sum_{k=1}^{i-1} \tilde{\Psi}_k^2 + \frac{l}{2p} \sum_{k=1}^{i-1} \|\tilde{\theta}_k\|^2 + \gamma_k \sum_{k=1}^{i-1} \tilde{\theta}_k^T \hat{\theta}_k \end{aligned} \tag{35}$$

Subsequently, we will demonstrate that Equation (35) is satisfied at step i . The Lyapunov function is provided as

$$V_i = V_{i-1} + \pi_i + \frac{1}{2} \tilde{\theta}_i^T \tilde{\theta}_i + \frac{1}{2} \tilde{\Psi}_i^2 \tag{36}$$

where $\pi_i = \int_{\sigma_i}^{x_i} \text{sig}^{2-\tau_{i+1}}(\text{sig}^{1/\tau_i}(s) - \text{sig}^{1/\tau_i}(\sigma_i)) ds$.

According to Equation (36), we obtain

$$\dot{V}_i = \dot{V}_{i-1} + \text{sig}^{2-\tau_{i+1}}(\vartheta_i) \dot{x}_i + \sum_{k=1}^{i-1} \frac{\partial \pi_i}{\partial x_k} \dot{x}_k + \sum_{k=1}^{i-1} \frac{\partial \pi_i}{\partial \text{sig}^{1/\tau_i}(\sigma_i)} \frac{d \text{sig}^{1/\tau_i}(\sigma_i)}{dt} - \tilde{\theta}_i^T \dot{\hat{\theta}}_i - \tilde{\Psi}_i \dot{\hat{\Psi}}_i \tag{37}$$

Invoking Equation (35), it is shown that

$$\begin{aligned} \dot{V}_i \leq & -\psi \sum_{k=1}^{i-1} \vartheta_k^2 - 2^{3\beta-2} \sum_{k=1}^{i-1} |\vartheta_k|^\eta + \tilde{\chi}(\ell \sum_{k=1}^{i-1} \vartheta_k^2 - \hat{\chi}) + (i-1)\Gamma_1 + \sum_{k=1}^{i-1} \tilde{\Psi}_k(\Psi_k - \delta_k \tilde{\Psi}_k) \\ & + (1 + \frac{p}{2} \delta_k^2) \sum_{k=1}^{i-1} \tilde{\Psi}_k^2 + \frac{l}{2p} \sum_{k=1}^{i-1} \|\tilde{\theta}_k\|^2 + \gamma_k \sum_{k=1}^{i-1} \tilde{\theta}_k^T \hat{\theta}_k + \text{sig}^{2-\tau_{i+1}}(\vartheta_i)(f_i(\bar{x}_i) + d_i(t)) \\ & + \text{sig}^{2-\tau_{i+1}}(\vartheta_i)(x_{i+1} - \sigma_{i+1}) + \text{sig}^{2-\tau_{i+1}}(\vartheta_i)\sigma_{i+1} + \sum_{k=1}^{i-1} \frac{\partial \pi_i}{\partial x_k} \dot{x}_k \\ & + \sum_{k=1}^{i-1} \frac{\partial \pi_i}{\partial \text{sig}^{1/\tau_k}(\sigma_k)} \frac{d \text{sig}^{1/\tau_k}(\sigma_k)}{dt} - \tilde{\theta}_i^T \dot{\hat{\theta}}_i - \tilde{\Psi}_i \dot{\hat{\Psi}}_i \end{aligned} \tag{38}$$

In addition, according to the definition of π_i , one has

$$\begin{aligned} \frac{\partial \pi_i}{\partial \text{sig}^{1/\tau_k}(\sigma_k)} \frac{d \text{sig}^{1/\tau_k}(\sigma_k)}{dt} & \leq (2 - \tau_{i+1}) \left| \frac{\partial \text{sig}^{1/\tau_k}(\sigma_k)}{\partial t} \right| \left| \int_{\sigma_i}^{x_i} \text{sig}^{1-\tau_{i+1}}(\text{sig}^{1/\tau_i}(s) - \text{sig}^{1/\tau_i}(\sigma_i)) ds \right| \\ & \leq (2 - \tau_{i+1}) \left| \frac{\partial \sigma_k^{1/\tau_k}}{\partial t} \right| |\vartheta_i|^{1-\tau_{i+1}} |x_i - \sigma_i| \\ & \leq 2(2 - \tau_{i+1}) |\vartheta_i|^{1-b} \left| \frac{\partial \sigma_k^{1/\tau_k}}{\partial t} \right| \end{aligned} \tag{39}$$

Similar to Equation (39), we have

$$\frac{\partial \pi_i}{\partial x_k} \dot{x}_k \leq 2(2 - \tau_{i+1}) |\vartheta_i|^{1-b} \left| \frac{\partial \sigma_k^{1/\tau_k}}{\partial x_k} \dot{x}_k \right| \tag{40}$$

Substituting Equations (39) and (40) into Equation (38) yields

$$\begin{aligned} \dot{V}_i \leq & -\psi \sum_{k=1}^{i-1} \vartheta_k^2 - 2^{3\beta-2} \sum_{k=1}^{i-1} |\vartheta_k|^\eta + \tilde{\chi}(\ell \sum_{k=1}^{i-1} \vartheta_k^2 - \hat{\chi}) + (i-1)\Gamma_1 + \sum_{k=1}^{i-1} \tilde{\Psi}_k(\Psi_k - \delta_k \tilde{\Psi}_k) \\ & + (1 + \frac{p}{2} \delta_k^2) \sum_{k=1}^{i-1} \tilde{\Psi}_k^2 + \frac{l}{2p} \sum_{k=1}^{i-1} \|\tilde{\theta}_k\|^2 + \gamma_k \sum_{k=1}^{i-1} \tilde{\theta}_k^T \hat{\theta}_k + \text{sig}^{2-\tau_{i+1}}(\vartheta_i)(f_i(\bar{x}_i) + d_i(t)) \\ & + \varsigma |\vartheta_{i+1}|^2 + \vartheta_i^2 + \text{sig}^{2-\tau_{i+1}}(\vartheta_i)\sigma_{i+1} + \text{sig}^{1-b}(\vartheta_i)\Omega_i(\bar{x}_i, \sigma_i) - \tilde{\theta}_i^T \dot{\hat{\theta}}_i - \tilde{\Psi}_i \dot{\hat{\Psi}}_i \end{aligned} \tag{41}$$

where $\Omega_i(\bar{x}_i, \sigma_{i+1}) = 2\text{sign}(\vartheta_i)(2 - \tau_{i+1})(\sum_{k=1}^{i-1} |\frac{\partial \sigma_i^{1/\tau_i}}{\partial t}| + \sum_{k=1}^{i-1} |\frac{\partial \sigma_i^{1/\tau_i}}{\partial x_k} \dot{x}_k|) + \text{sig}^{b-1}(\vartheta_i)\zeta|\vartheta_{i+1}|^2$.
In a manner akin to Equation (27), one has

$$\text{sig}^{1-b}(\vartheta_i)\Omega_i \leq |\vartheta_i|^{1-b} \hbar_i^{\frac{1-b}{2}} \leq \ell_i \vartheta_i^2 \chi^* + \Gamma_1 \quad (42)$$

where $\hbar_i = (\sqrt{2}\|\tilde{\theta}_{\Omega_i}\|)^{2/(1-b)}$.

The FLSs serve as an approximator to identify $f_i(\bar{x}_i)$, such that $f_i(\bar{x}_i) = \theta_i^T \varphi_i + \epsilon_i$ with $\bar{\epsilon}_i \geq |\epsilon_i|$. Defining $\Psi_i = d_i(t) + \bar{\epsilon}_i$, the disturbance observer is formulated with δ_i as follows

$$\begin{aligned} \dot{\Psi}_i &= \delta_i(x_i - \phi_i) \\ \dot{\phi}_i &= x_{i+1} + \hat{\theta}_i^T \varphi_i + \hat{\Psi}_i \end{aligned} \quad (43)$$

We design the virtual controller and update laws as

$$\sigma_{i+1} = -\text{sig}^{\tau_{i+1}}(\vartheta_i)(\ell \hat{\chi} + 1 + \psi) - \frac{1}{4} \text{sig}^{2-\tau_{i+1}}(\vartheta_i) - \hat{\theta}_i^T \varphi_i - \hat{\Psi}_i - 2^{3\beta-2} |\vartheta_i|^\eta \text{sig}^{\tau_{i+1}-2}(\vartheta_i) \quad (44)$$

$$\hat{\theta}_i = \text{sig}^{2-\tau_{i+1}}(\vartheta_i) \varphi_i - \gamma_i \hat{\theta}_i \quad (45)$$

where $\gamma_i > 0$ a is designed parameter.

Invoking Equation (42) to Equation (45), one obtains

$$\begin{aligned} \dot{V}_i &\leq -\psi \sum_{k=1}^i \vartheta_k^2 - 2^{3\beta-2} \sum_{k=1}^i |\vartheta_k|^\eta + \tilde{\chi}(\ell \sum_{k=1}^i \vartheta_k^2 - \hat{\chi}) + i\Gamma_1 + \sum_{k=1}^i \tilde{\Psi}_k(\dot{\Psi}_k - \delta_k \tilde{\Psi}_k) \\ &\quad + (1 + \frac{p}{2} \delta_k^2) \sum_{k=1}^i \tilde{\Psi}_k^2 + \frac{l}{2p} \sum_{k=1}^i \|\tilde{\theta}_k\|^2 + \gamma_k \sum_{k=1}^i \tilde{\theta}_k^T \hat{\theta}_k \end{aligned} \quad (46)$$

Step n : The Lyapunov function is defined as

$$V_n = V_{n-1} + \pi_n + \frac{1}{2} \tilde{\theta}_n^T \tilde{\theta}_n + \frac{1}{2} \tilde{\Psi}_n^2 \quad (47)$$

According to Equation (47), we obtain

$$\begin{aligned} \dot{V}_n &= \dot{V}_{n-1} + \text{sig}^{2-\tau_{n+1}}(\vartheta_n) \dot{x}_n + \sum_{k=1}^n \frac{\partial \pi_n}{\partial x_k} \dot{x}_k + \sum_{k=1}^n \frac{\partial \pi_n}{\partial \text{sig}^{1/\tau_k}(\sigma_k)} \frac{d \text{sig}^{1/\tau_k}(\sigma_k)}{dt} - \tilde{\theta}_n^T \dot{\hat{\theta}}_n - \tilde{\Psi}_n \dot{\hat{\Psi}}_n \\ &= \dot{V}_{n-1} + \text{sig}^{2-\tau_{n+1}}(\vartheta_n)(u(t) + d_n(t) + f_n(\bar{x}_n)) + \sum_{k=1}^n \frac{\partial \pi_n}{\partial x_k} \dot{x}_k \\ &\quad + \sum_{k=1}^n \frac{\partial \pi_n}{\partial \text{sig}^{1/\tau_k}(\sigma_k)} \frac{d \text{sig}^{1/\tau_k}(\sigma_k)}{dt} - \tilde{\theta}_n^T \dot{\hat{\theta}}_n - \tilde{\Psi}_n \dot{\hat{\Psi}}_n \end{aligned} \quad (48)$$

Based on Equation (46), we have

$$\begin{aligned}
\dot{V}_n &\leq -\psi \sum_{k=1}^{n-1} \vartheta_k^2 - 2^{3\beta-2} \sum_{k=1}^{n-1} |\vartheta_k|^\eta + \tilde{\chi}(\ell \sum_{k=1}^{n-1} \vartheta_k^2 - \hat{\chi}) + (n-1)\Gamma_1 + \sum_{k=1}^{n-1} \tilde{\Psi}_k(\Psi_k - \delta_k \tilde{\Psi}_k) \\
&\quad + (1 + \frac{p}{2} \delta_k^2) \sum_{k=1}^{n-1} \tilde{\Psi}_k^2 + \frac{l}{2p} \sum_{k=1}^{n-1} \|\tilde{\theta}_k\|^2 + \gamma_k \sum_{k=1}^{n-1} \tilde{\theta}_k^T \hat{\theta}_k + \text{sig}^{2-\tau_{n+1}}(\vartheta_n)(u(t) + d_n(t)) \\
&\quad + f_n(\bar{x}_n) + \sum_{k=1}^n \frac{\partial \pi_n}{\partial x_k} \dot{x}_k + \sum_{k=1}^n \frac{\partial \pi_n}{\partial \text{sig}^{1/\tau_k}(\sigma_k)} \frac{d \text{sig}^{1/\tau_k}(\sigma_k)}{dt} - \tilde{\theta}_n^T \hat{\theta}_n - \tilde{\Psi}_n \dot{\Psi}_n \\
&\leq -\psi \sum_{k=1}^{n-1} \vartheta_k^2 - 2^{3\beta-2} \sum_{k=1}^{n-1} |\vartheta_k|^\eta + \tilde{\chi}(\ell \sum_{k=1}^{n-1} \vartheta_k^2 - \hat{\chi}) + (n-1)\Gamma_1 + \sum_{k=1}^{n-1} \tilde{\Psi}_k(\Psi_k - \delta_k \tilde{\Psi}_k) \\
&\quad + (1 + \frac{p}{2} \delta_k^2) \sum_{k=1}^{n-1} \tilde{\Psi}_k^2 + \frac{l}{2p} \sum_{k=1}^{n-1} \|\tilde{\theta}_k\|^2 + \gamma_k \sum_{k=1}^{n-1} \tilde{\theta}_k^T \hat{\theta}_k + \text{sig}^{2-\tau_{n+1}}(\vartheta_n)(u(t) + d_n(t)) \\
&\quad + f_n(\bar{x}_n) + \text{sig}^{1-b}(\vartheta_n) \Omega_n(\bar{x}_n, \sigma_n) - \tilde{\theta}_n^T \hat{\theta}_n - \tilde{\Psi}_n \dot{\Psi}_n
\end{aligned} \tag{49}$$

where $\Omega_n(\bar{x}_n, \sigma_n) = 2\text{sig}(\vartheta_n)(2 - \tau_{n+1}) \left(\sum_{k=1}^n \left| \frac{\partial \sigma_k^{1/\tau_k}}{\partial t} \right| + \sum_{k=1}^n \left| \frac{\partial \sigma_k^{1/\tau_k}}{\partial x_k} \dot{x}_k \right| \right)$.

In a manner akin to Equation (27), we have

$$\text{sig}^{1-b}(\vartheta_n) \Omega_n \leq |\vartheta_n|^{1-b} \hat{h}_n^{1-b} \leq \ell_n \vartheta_n^2 \chi^* + \Gamma_1 \tag{50}$$

where $\hat{h}_n = (\sqrt{2} \|\tilde{\theta}_{\Omega_n}\|)^{2/(1-b)}$.

The FLSs serve as an approximator to identify $f_n(\bar{x}_n)$, such that $f_n(\bar{x}_n) = \theta_n^T \varphi_n + \epsilon_n$ with $\bar{\epsilon}_n \geq |\epsilon_n|$. Defining $\Psi_n = d_n(t) + \bar{\epsilon}_n$, the disturbance observer is formulated with δ_n as follows

$$\begin{aligned}
\dot{\Psi}_n &= \delta_n(x_n - \phi_n) \\
\dot{\phi}_n &= \hat{\theta}_n^T \varphi_n + \hat{\Psi}_i
\end{aligned} \tag{51}$$

The actual controller and update laws are defined as

$$u(t) = -\text{sig}^{\tau_{n+1}}(\vartheta_n)(\ell \hat{\chi} + \psi) - \frac{1}{4} \text{sig}^{2-\tau_{n+1}}(\vartheta_n) - \hat{\theta}_n^T \varphi_n - \hat{\Psi}_n - 2^{3\beta-2} |\vartheta_n|^\eta \text{sig}^{\tau_{n+1}-2}(\vartheta_n) \tag{52}$$

$$\hat{\theta}_n = \text{sig}^{2-\tau_{n+1}}(\vartheta_n) \varphi_n - \gamma_n \hat{\theta}_n \tag{53}$$

$$\hat{\chi} = \ell \sum_{i=1}^n \vartheta_i^2 - \mu \psi \hat{\chi} \tag{54}$$

Invoking Equation (50) to Equation (54) yields

$$\begin{aligned}
\dot{V}_n &\leq -\psi \sum_{k=1}^n \vartheta_k^2 - 2^{3\beta-2} \sum_{k=1}^n |\vartheta_k|^\eta + \tilde{\chi}(\ell \sum_{k=1}^n \vartheta_k^2 - \hat{\chi}) + n\Gamma_1 + \sum_{k=1}^n \tilde{\Psi}_k(\Psi_k - \delta_k \tilde{\Psi}_k) \\
&\quad + (1 + \frac{p}{2} \delta_k^2) \sum_{k=1}^n \tilde{\Psi}_k^2 + \frac{l}{2p} \sum_{k=1}^n \|\tilde{\theta}_k\|^2 + \gamma_k \sum_{k=1}^n \tilde{\theta}_k^T \hat{\theta}_k \\
&\leq -\psi \sum_{k=1}^n \vartheta_k^2 - 2^{3\beta-2} \sum_{k=1}^n |\vartheta_k|^\eta + \mu \psi \tilde{\chi} \hat{\chi} + n\Gamma_1 + \sum_{k=1}^n \tilde{\Psi}_k(\Psi_k - \delta_k \tilde{\Psi}_k) \\
&\quad + (1 + \frac{p}{2} \delta_k^2) \sum_{k=1}^n \tilde{\Psi}_k^2 + \frac{l}{2p} \sum_{k=1}^n \|\tilde{\theta}_k\|^2 + \gamma_k \sum_{k=1}^n \tilde{\theta}_k^T \hat{\theta}_k
\end{aligned} \tag{55}$$

Based on Lemma 2, for any $b_1 > (1/2)$ and $b_2 > (1/2)$, we have

$$\mu\psi\tilde{\chi}\hat{\chi} = -\mu\psi\tilde{\chi}(\tilde{\chi} - \chi^*) \leq -\frac{c_1\psi}{2}\tilde{\chi}^2 + \frac{b_1\psi\mu}{2}\chi^{*2} \tag{56}$$

$$\gamma_k\tilde{\theta}_k^T\hat{\theta}_k \leq -\frac{\gamma_k(2b_2 - 1)}{2b_2}\|\tilde{\theta}_k\|^2 + \frac{b_2\gamma_k}{2}\|\theta_k\|^2 \tag{57}$$

where $c_1 = 2^{\frac{\mu(b_1-0.5)}{b_1}}$.

Substituting Equations (56) and (57) into Equation (55), we have

$$\begin{aligned} \dot{V}_n &\leq -\psi \sum_{k=1}^n \vartheta_k^2 - 2^{3\beta-2} \sum_{k=1}^n |\vartheta_k|^\eta - \frac{c_1\psi}{2}\tilde{\chi}^2 + \frac{b_1\psi\mu}{2}\chi^{*2} + n\Gamma_1 + \sum_{k=1}^n \tilde{\Psi}_k(\Psi_k - \delta_k\tilde{\Psi}_k) \\ &\quad + (1 + \frac{p}{2}\delta_k^2) \sum_{k=1}^n \tilde{\Psi}_k^2 + \frac{l}{2p} \sum_{k=1}^n \|\tilde{\theta}_k\|^2 - \sum_{k=1}^n \frac{\gamma_k(2b_2 - 1)}{2b_2}\|\tilde{\theta}_k\|^2 + \sum_{k=1}^n \frac{b_2\gamma_k}{2}\|\theta_k\|^2 \\ &\leq -\psi \sum_{k=1}^n \vartheta_k^2 - 2^{3\beta-2} \sum_{k=1}^n |\vartheta_k|^\eta - \frac{c_1\psi}{2}\tilde{\chi}^2 + \frac{b_1\psi\mu}{2}\chi^{*2} + n\Gamma_1 - \varrho_{1,k} \sum_{k=1}^n \tilde{\Psi}_k^2 \\ &\quad - \varrho_{2,k} \sum_{k=1}^n \|\tilde{\theta}_k\|^2 + \sum_{k=1}^n \frac{b_2\gamma_k}{2}\|\theta_k\|^2 \end{aligned} \tag{58}$$

where $\varrho_{1,k} = \delta_k - 1 - \frac{p}{2}\delta_k^2$ and $\varrho_{2,k} = \frac{\gamma_k(2b_2-1)}{2b_2} - \frac{l}{2p}$.

3.2. Stability Analysis

From the analysis above, the primary theorem of this paper will be articulated as follows.

Theorem 1. Consider the nonlinear systems in Equation (1), the actual fixed-time adaptive fuzzy control strategy in Equation (52) is proposed with the virtual control laws in Equations (20), (30), and (44), the adaptation laws of Equations (21), (31), (45), (53), and (54), and the disturbances observers of Equations (22), (32), (43), and (51). The derived control scheme can ensure that the resulting system is practically fixed-time stable, and the states x_i converge in the region $|x_i| \leq \Delta_x = \min\{\omega_1^{-\frac{1}{\alpha}}(\frac{Y}{1-\eta_0})^{\frac{1}{\alpha}}, \bar{\omega}_2^{-\frac{1}{\alpha}}(\frac{Y}{1-\eta_0})^{\frac{1}{\beta}}\}$ in fixed time $T \leq \frac{1}{\omega_1\eta_0(1-\alpha)} + \frac{1}{\bar{\omega}_2\eta_0(\beta-1)}$, where $\omega_1 = \min\{\psi/2, c_1\psi/2n^{1-\beta}, \varrho_{1,k}, \varrho_{2,k}\}$, $c_1 = 2^{\frac{\mu(b_1-0.5)}{b_1}}$, $b_1 > (1/2)$, $b_2 > (1/2)$, $1 > \eta_0 > 0$, $Y = \omega_\exists + n\Gamma_1 + \omega_\theta + \omega_\Psi + \sum_{k=1}^n \frac{b_2\gamma_k}{2}\|\theta_k\|^2 + \omega_\exists + \frac{b_1\psi\mu}{2}\chi^{*2}$, $\bar{\omega}_2 = \min\{2^{\beta-1}, c_1^\beta\psi^\beta/2^\beta n^{1-\beta}, \varrho_{1,k}^\beta/n^{\beta-1}, \varrho_{2,k}^\beta n^{\beta-1}\}$.

Proof. From Equation (47), V_n can be rewritten as

$$V_n = \sum_{k=1}^n \pi_k + \frac{1}{2}\tilde{\chi}^2 + \frac{1}{2} \sum_{k=1}^n \tilde{\theta}_k^T\tilde{\theta}_k + \frac{1}{2} \sum_{k=1}^n \tilde{\Psi}_k^2 \tag{59}$$

where

$$\sum_{k=1}^n \pi_k = \sum_{k=1}^n \int_{\sigma_j}^{x_k} \text{sig}^{2-\tau_{k+1}}(\text{sig}^{1/\tau_k}(s) - \text{sig}^{1/\tau_k}(\sigma_k)) ds \leq 2 \sum_{k=1}^n |\vartheta_k|^{2-b} \tag{60}$$

Furthermore, we have

$$\left(\sum_{k=1}^n \pi_k\right)^\alpha \leq \left(2 \sum_{k=1}^n |\vartheta_k|^{2-b}\right)^\alpha \leq 2 \sum_{k=1}^n \vartheta_k^2 \tag{61}$$

$$\left(\sum_{k=1}^n \pi_k\right)^\beta \leq \left(2 \sum_{k=1}^n |\vartheta_k|^{2-b}\right)^\beta \leq 2^{\beta-1} \sum_{k=1}^n (2|\vartheta_k|^{2-b})^\beta \leq \frac{2^{2\beta-1}}{n^{1-\beta}} \sum_{k=1}^n |\vartheta_k|^\eta \quad (62)$$

where $0 < \alpha = \frac{2}{2-b} < 1$, $\eta > 2 - b$, $\beta = \frac{\eta}{2-b} > 1$.

Based on [43], it is known that, for a bounded function $\tilde{\chi}$ with constant Δ_χ as the boundary, $0 < \alpha < 1$ and $\beta > 1$, such that

$$-\frac{c_1\psi}{2}\tilde{\chi}^2 \leq -\left(\frac{c_1\psi}{4}\tilde{\chi}^2\right)^\alpha - \left(\frac{c_1\psi}{4}\tilde{\chi}^2\right)^\beta + \omega_\mathfrak{S} \quad (63)$$

where $\omega_\mathfrak{S} = (1 - \alpha)\alpha^{\alpha/1-\alpha} + \left(\frac{c_1\psi}{4}\Delta_\chi^2\right)^\beta$.

Similar to

$$-q_{2,k} \sum_{k=1}^n \|\tilde{\theta}_k\|^2 \leq -\left(\frac{q_{2,k}}{2} \sum_{k=1}^n \|\tilde{\theta}_k\|^2\right)^\alpha - \frac{1}{n^{\beta-1}} \left(\frac{q_{2,k}}{2} \sum_{k=1}^n \|\tilde{\theta}_k\|^2\right)^\beta + \omega_\theta \quad (64)$$

where $\omega_\theta = (1 - \alpha)\alpha^{\alpha/1-\alpha} + \sum_{k=1}^n \left(\frac{q_{2,k}}{2} \Delta_{\theta,k}^2\right)^\beta$.

$$-q_{1,k} \sum_{k=1}^n \tilde{\Psi}_k^2 \leq -\left(\frac{q_{2,k}}{2} \sum_{k=1}^n \tilde{\Psi}_k^2\right)^\alpha - \frac{1}{n^{\beta-1}} \left(\frac{q_{1,k}}{2} \sum_{k=1}^n \tilde{\Psi}_k^2\right)^\beta + \omega_\Psi \quad (65)$$

where $\omega_\Psi = (1 - \alpha)\alpha^{\alpha/1-\alpha} + \sum_{k=1}^n \left(\frac{q_{1,k}}{2} \Delta_{\Psi,k}^2\right)^\beta$.

Then, combining Equation (58) and Equations (63)–(65), we have

$$\begin{aligned} \dot{V}_n &\leq -\psi \sum_{k=1}^n \vartheta_k^2 - 2^{3\beta-2} \sum_{k=1}^n |\vartheta_k|^\eta - \left(\frac{c_1\psi}{4}\tilde{\chi}^2\right)^\alpha - \left(\frac{c_1\psi}{4}\tilde{\chi}^2\right)^\beta + \omega_\mathfrak{S} + \frac{b_1\psi\mu}{2}\chi^{*2} \\ &\quad + n\Gamma_1 - \left(\frac{q_{2,k}}{2} \sum_{k=1}^n \|\tilde{\theta}_k\|^2\right)^\alpha - \frac{1}{n^{\beta-1}} \left(\frac{q_{2,k}}{2} \sum_{k=1}^n \|\tilde{\theta}_k\|^2\right)^\beta + \omega_\theta \\ &\quad - \left(\frac{q_{2,k}}{2} \sum_{k=1}^n \tilde{\Psi}_k^2\right)^\alpha - \frac{1}{n^{\beta-1}} \left(\frac{q_{1,k}}{2} \sum_{k=1}^n \tilde{\Psi}_k^2\right)^\beta + \omega_\Psi + \sum_{k=1}^n \frac{b_2\gamma_k}{2} \|\theta_k\|^2 \\ &\leq -\omega_1 \left\{ \left(\sum_{k=1}^n \omega_k\right)^\alpha + \left(\frac{1}{2}\tilde{\chi}^2\right)^\alpha + \left(\frac{1}{2} \sum_{k=1}^n \tilde{\Psi}_k^2\right)^\alpha + \left(\frac{1}{2} \sum_{k=1}^n \|\tilde{\theta}_k\|^2\right)^\alpha \right\} \\ &\quad - \omega_2 \left\{ \left(\sum_{k=1}^n \omega_k\right)^\beta + \left(\frac{1}{2}\tilde{\chi}^2\right)^\beta + \left(\frac{1}{2} \sum_{k=1}^n \tilde{\Psi}_k^2\right)^\beta + \left(\frac{1}{2} \sum_{k=1}^n \|\tilde{\theta}_k\|^2\right)^\beta \right\} + Y \end{aligned} \quad (66)$$

where $\omega_1 = \min\{\psi/2, c_1\psi/2n^{1-\beta}, q_{1,k}, q_{2,k}\}$, $\omega_2 = \min\{2^{\beta-1}, c_1^\beta\psi^\beta/2^\beta n^{1-\beta}, q_{1,k}^\beta/n^{\beta-1}, q_{2,k}^\beta n^{\beta-1}\}$, $Y = \omega_\mathfrak{S} + n\Gamma_1 + \omega_\theta + \omega_\Psi + \sum_{k=1}^n \frac{b_2\gamma_k}{2} \|\theta_k\|^2 + \omega_\mathfrak{S} + \frac{b_1\psi\mu}{2}\chi^{*2}$.

Furthermore, based on Lemma 1, we have

$$\begin{aligned} \dot{V}_n &\leq -\omega_1 \left[\sum_{k=1}^n \omega_k + \frac{1}{2}\tilde{\chi}^2 + \frac{1}{2} \sum_{k=1}^n \tilde{\Psi}_k^2 + \frac{1}{2} \sum_{k=1}^n \|\tilde{\theta}_k\|^2 \right]^\alpha \\ &\quad - \bar{\omega}_2 \left[\sum_{k=1}^n \omega_k + \frac{1}{2}\tilde{\chi}^2 + \frac{1}{2} \sum_{k=1}^n \tilde{\Psi}_k^2 + \frac{1}{2} \sum_{k=1}^n \|\tilde{\theta}_k\|^2 \right]^\beta + Y \\ &\leq -\omega_1 V_n^\alpha - \bar{\omega}_2 V_n^\beta + Y \end{aligned} \quad (67)$$

where $\bar{\omega}_2 = n^{1-\beta}\omega_2$.

In accordance with Lemma 4, Equation (1) demonstrates practical fixed-time stability. Moreover, x_i will converge in the region

$$B = \left\{ \lim_{t \rightarrow T_s} x_i | V_n \leq \min \left\{ \omega_1^{-\frac{1}{\alpha}} \left(\frac{Y}{1-\eta_0} \right)^{\frac{1}{\alpha}}, \bar{\omega}_2^{-\frac{1}{\beta}} \left(\frac{Y}{1-\eta_0} \right)^{\frac{1}{\beta}} \right\} \right\} \quad (68)$$

$$\text{in } T \leq \frac{1}{\omega_1 \eta_0 (1-\alpha)} + \frac{1}{\omega_2 \eta_0 (\beta-1)}. \quad \square$$

The block diagram of the proposed adaptive fixed-time controller is shown in Figure 1.

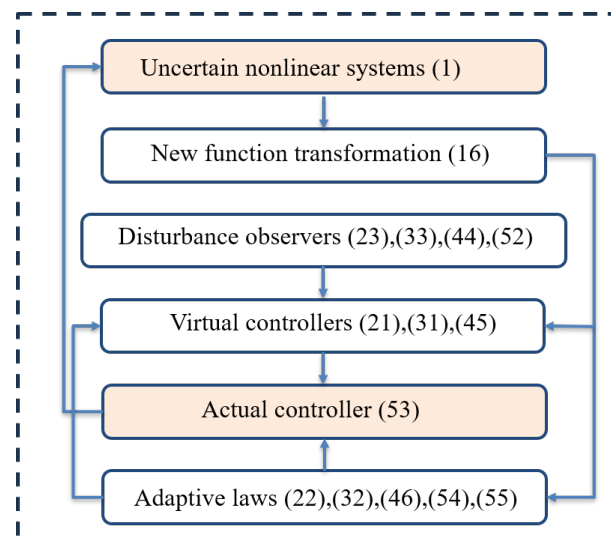


Figure 1. Block diagram of the fixed-time control scheme.

Remark 2. In this article, we present a fixed-time adaptive fuzzy control protocol for uncertain nonlinear systems. It is crucial to highlight that our proposed controller, in contrast to finite-time controllers, ensures the practical fixed-time stability of controlled systems. Furthermore, we employ the backstepping technique and adding one power integrator for developing the fixed-time controller, avoiding noncontinuous and singular issues.

Remark 3. This paper presents a fixed-time fuzzy adaptive controller designed for uncertain nonlinear systems with mismatched disturbances. Distinguishing itself from finite-time controllers [20,21,33], our proposed controller guarantees practical fixed-time stability of closed-loop systems, with the convergence time unaffected by the initial conditions. Thus, compared to finite-time control, fixed-time control is more applicable to practical engineering. In contrast to the fixed-time controllers in [34,36,37], our method considers mismatched disturbances. Additionally, we have developed a dedicated disturbance observer to address these mismatches, thereby improving the system's robustness and control precision. Leveraging property $0 < \varphi^T \varphi \leq 1$, our proposed control scheme relies on only one adaptive parameter χ related to the maximum norm of the fuzzy weight parameters, eliminating the need for directly incorporating multiple fuzzy weight parameters. This approach significantly reduces the computational load. In upcoming research, we will further reduce the computational load of the system by introducing an event-triggered mechanism.

The design algorithm of the proposed adaptive fixed-time controller is shown in Algorithm 1.

Remark 4. In contrast to the event-triggered control protocols designed in [44,45], which necessitate the determination of upper bounds for system uncertainties, our control protocol is derived using an adaptive technique that does not have such a requirement. Additionally, refs. [44,45] do not address mismatched disturbances, whereas our proposed controller is capable of handling the more challenging task involving mismatched disturbances.

Remark 5. In this paper, a fixed-time fuzzy adaptive controller is proposed for uncertain nonlinear systems with mismatched disturbances. In order to mitigate the impact of mismatched disturbances, the disturbance observers (23), (33), (44), and (52) are designed. In both virtual controllers (21), (31), and (45) and actual controllers (53), we can observe the presence of the term $\hat{\Psi}_i$. This term is obtained through a disturbance observer and is utilized to mitigate the impact of disturbances on the system.

Algorithm 1 Algorithm to design fixed-time fuzzy controller

Input: The parameters τ_1, τ_i , and b in intermediate variables (16); the parameters $\ell > 0, \psi > 0$, and $\beta > 1$ in virtual control laws (21), (31), and (45) and actual controller (53); the parameters $\gamma_i > 0, \ell > 0, \mu > 0$, and $\psi > 0$ in adaptive laws (22), (32), (46), (54), and

(55); the parameter δ_i in disturbance observers (23), (33), (44), and (52).

Output: The fixed-time controller (53).

Begin:

1: Step 1: Establish a system model.

2: Step 2: Design the intermediate variables.

3: Step 3: Design the disturbance observers.

4: Step 4: Chose appropriate design parameters and design adaptive laws and virtual controllers.

5: Step 5: Select appropriate design parameters and design actual control law (53).

6: Step 6: Calculate the convergence time of the resulting closed-loop system.

end

4. Illustrative Examples

In this section, we conduct an illustrative example on the dynamics of a one-line arm to validate the effectiveness of the proposed controller, the system is described as

$$N\ddot{q} + M\dot{q} + R\sin(q) = F \quad (69)$$

where q represents the arm's position, F denotes the control input signal. $N = 1 \text{ kg} \cdot \text{m}^2$ refers to the mechanical inertia, $R = mgL$ with $L = 1 \text{ m}$ refers to the link length, $M = 1 \text{ kg} \cdot \text{m}^2$ denotes the mechanical inertia, $g = 10 \text{ N/kg}$ refers to the gravitational acceleration, and $m = 1 \text{ kg}$ represents the load mass.

Let $x_1 = q$ and $x_2 = \dot{q}$, $d_1 = 0.1\cos(x_1)\sin(x_2)$, and $d_2 = \sin(0.01t)$ into consideration; then, Equation (69) can be described by

$$\begin{aligned} \dot{x}_1 &= x_2 + d_1 \\ \dot{x}_2 &= -x_2 - 10\sin(x_1) + u + d_2 \end{aligned} \quad (70)$$

Case 1. The parameters are designed as $\psi = \frac{1}{16}$, $\ell = 0.5$, $\mu = 16$, $\delta_1 = 2$, $\Psi_1(0) = 0$, $\Psi_2(0) = 0$, $\gamma_2 = 1$, $\delta_2 = 2$, $b = -\frac{2}{7}$, $\tau_1 = 1$, $\tau_2 = \frac{5}{7}$, $\tau_3 = \frac{3}{7}$, $\beta = 1.1$, $x(0) = [0.5, -1.5]^T$, $\hat{\chi}(0) = 0.04$.

Case 2. The parameters are designed as $\psi = \frac{1}{16}$, $\ell = 0.4$, $\mu = 16$, $\delta_1 = 2$, $\hat{\chi}(0) = 0.02$, $\Psi_1(0) = 0$, $\Psi_2(0) = 0$, $\gamma_2 = 1$, $\delta_2 = 2$, $b = -\frac{2}{5}$, $\tau_1 = 1$, $\tau_2 = \frac{3}{5}$, $\tau_3 = \frac{1}{5}$, $x(0) = [-0.5, 1.5]^T$, and $\beta = 1.1$.

The simulation results for two cases are given by Figures 2–9. The trajectory of state x_1 for case 1 is given in Figure 2. The trajectory of state x_2 for case 1 is given in Figure 3. The trajectory of $\hat{\chi}$ for case 1 is provided in Figure 4. From Figures 2 and 3, it can be observed that, with the proposed fixed-time controller, the system states x_1 and x_2 for case 1 converge to near-zero within 4 s. The trajectory of state x_1 for case 2 is given in Figure 6. The trajectory of state x_2 for case 2 is given in Figure 7. From Figures 6 and 7, it can be observed that, with the proposed fixed-time controller, the system states x_1 and x_2 for case 2 converge to near-zero within 4 s. The trajectory of $\hat{\chi}$ for case 2 is provided in Figure 8. The trajectory of the control signal for the two cases are given in Figures 5 and 9, respectively.

In order to further investigate the performance of the designed controller, a set of comparative simulation validations was conducted employing a finite-time control approach. A finite-time controller without disturbance observed based on the classical back-stepping method is also applied to Equation (70). The finite-time controller is designed as

$$u(t) = -\text{sig}^{\tau_{n+1}}(\vartheta_n)(\ell\hat{\chi} + \psi) - \frac{1}{4}\text{sig}^{2-\tau_{n+1}}(\vartheta_n) - \hat{\vartheta}_n^T \varphi_n$$

where the adaptive laws are defined as

$$\begin{aligned}\dot{\hat{\theta}}_n &= \text{sig}^{2-\tau_{n+1}}(\vartheta_n)\varphi_n - \gamma_n\hat{\theta}_n \\ \dot{\hat{\chi}} &= \ell \sum_{i=1}^n \vartheta_i^2 - \mu\psi\hat{\chi}\end{aligned}$$

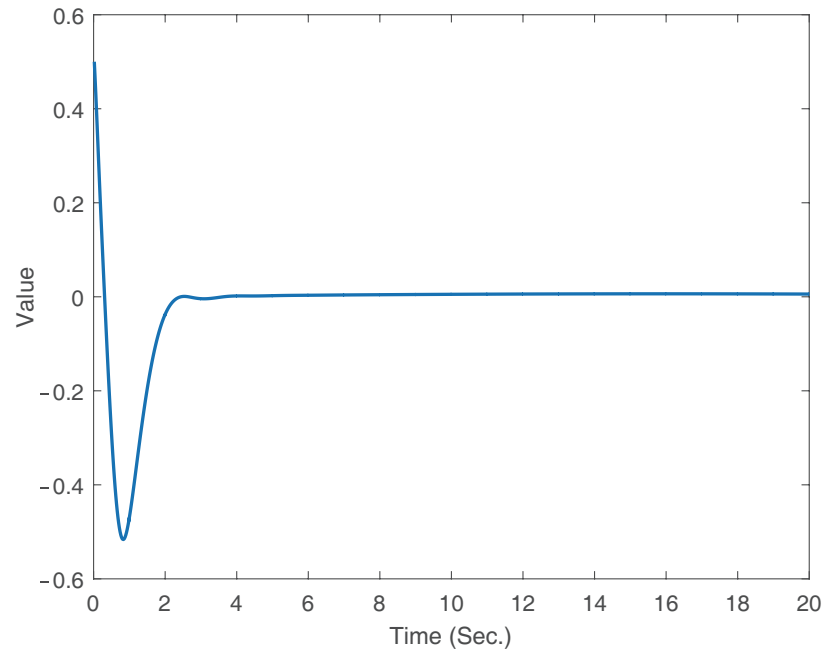


Figure 2. The trajectory of state x_1 for case 1.

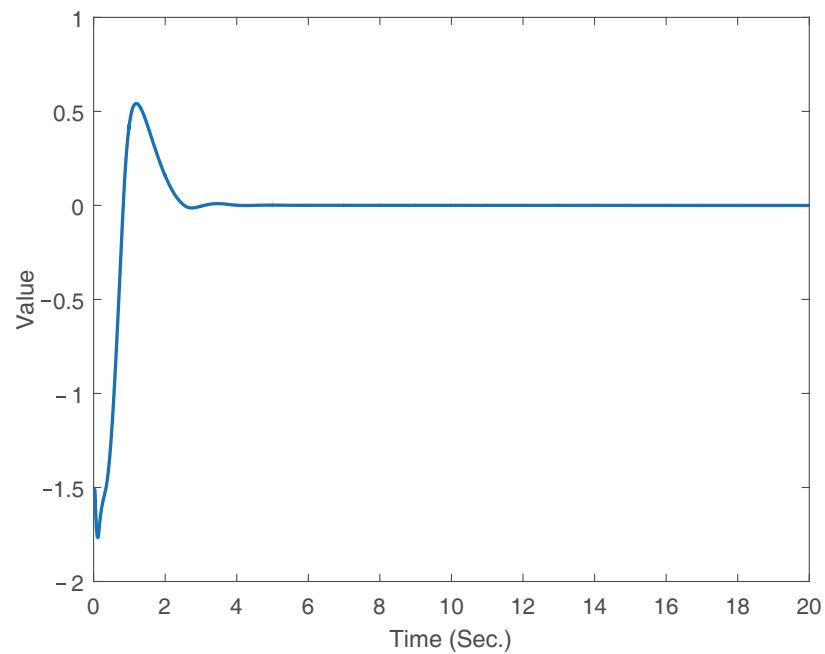


Figure 3. The trajectory of state x_2 for case 1.

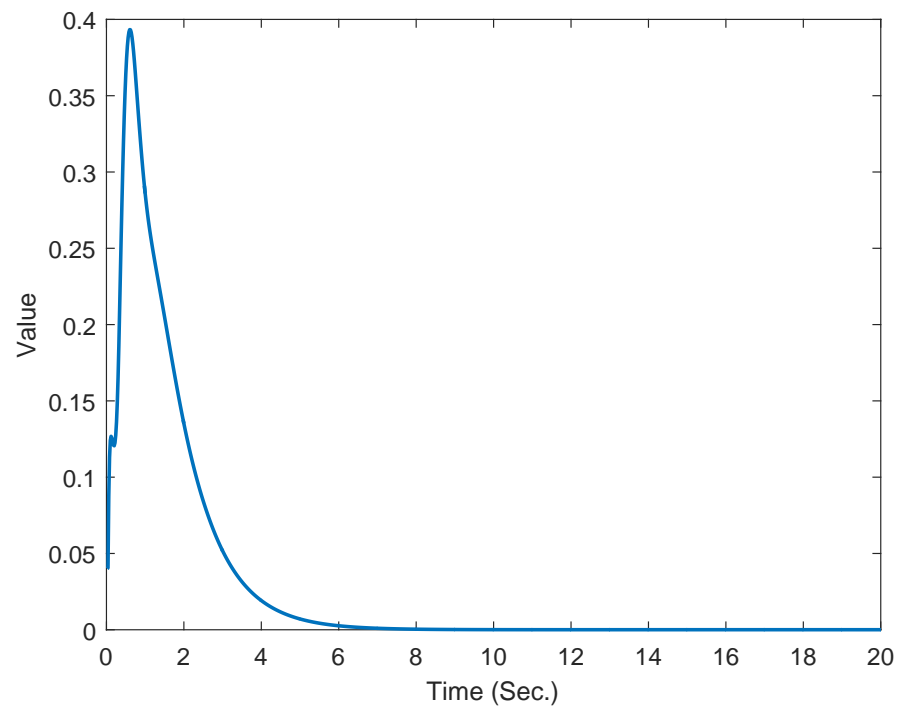


Figure 4. The trajectory of $\hat{\chi}$ for case 1.

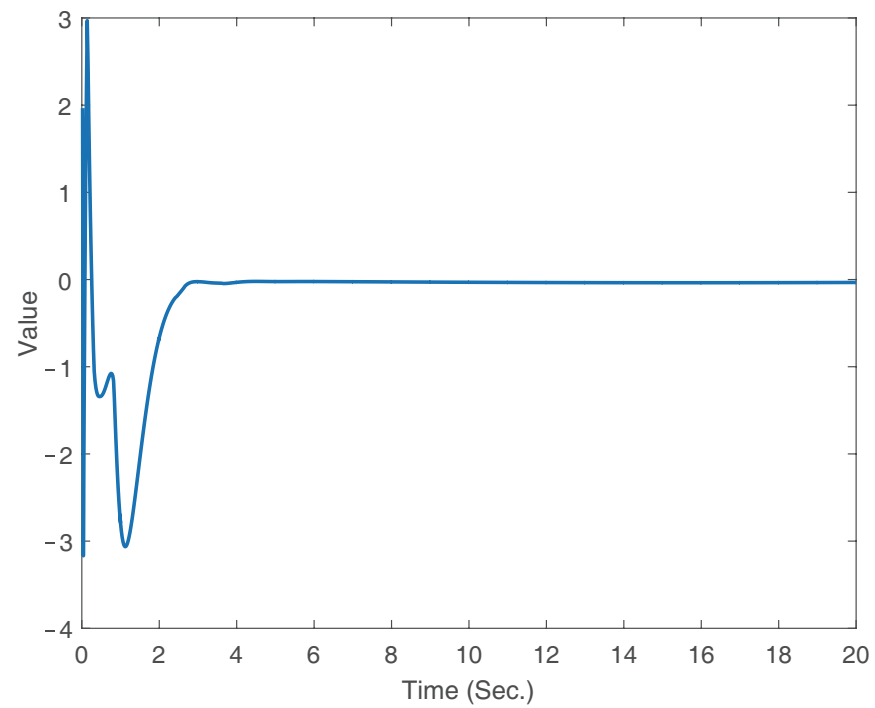


Figure 5. The trajectory of control signal for case 1.

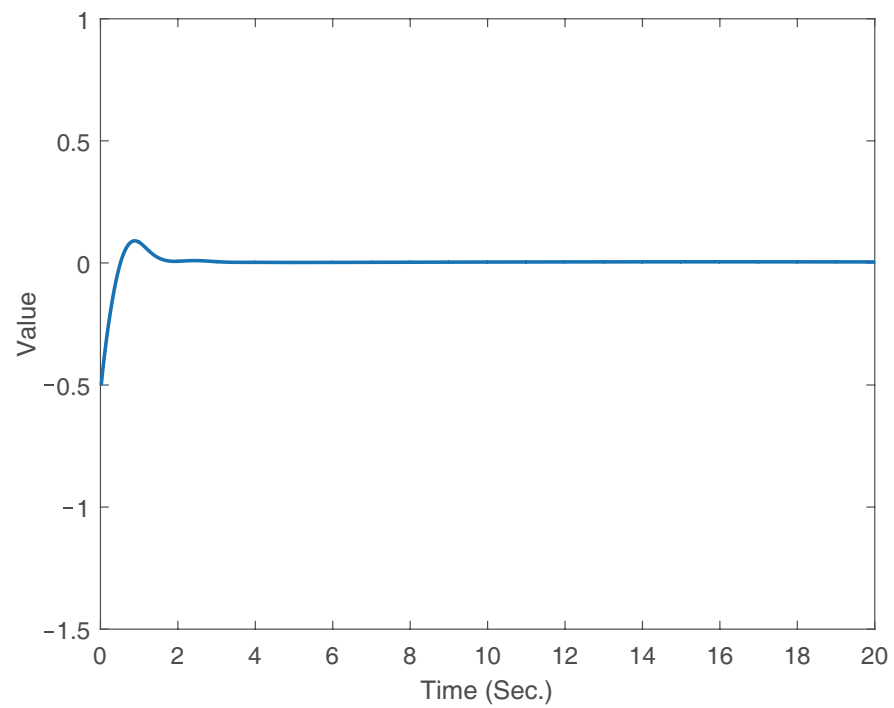


Figure 6. The trajectory of state x_1 for case 2.

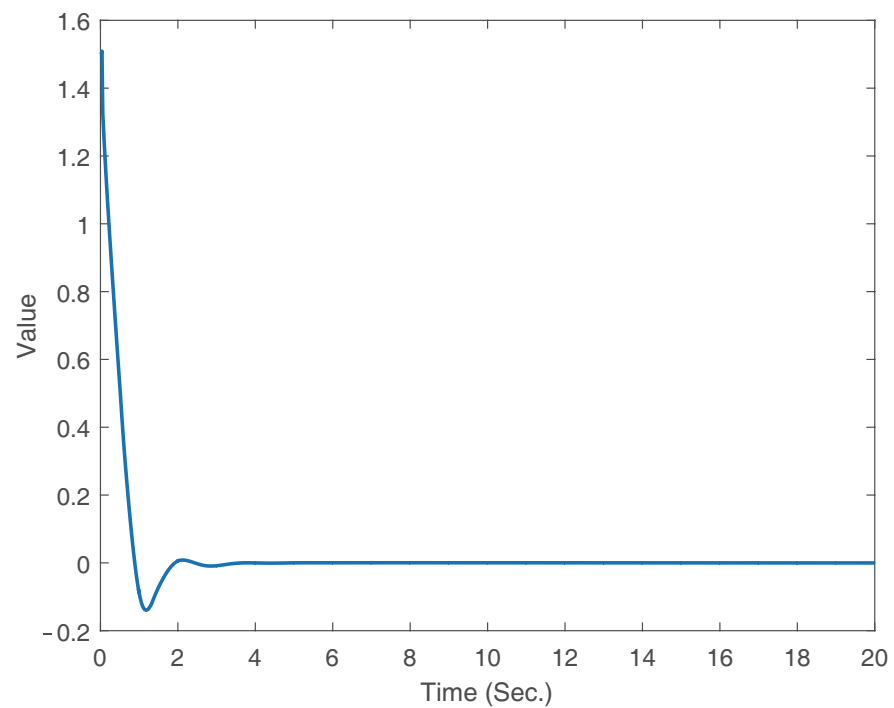


Figure 7. The trajectory of state x_2 for case 2.

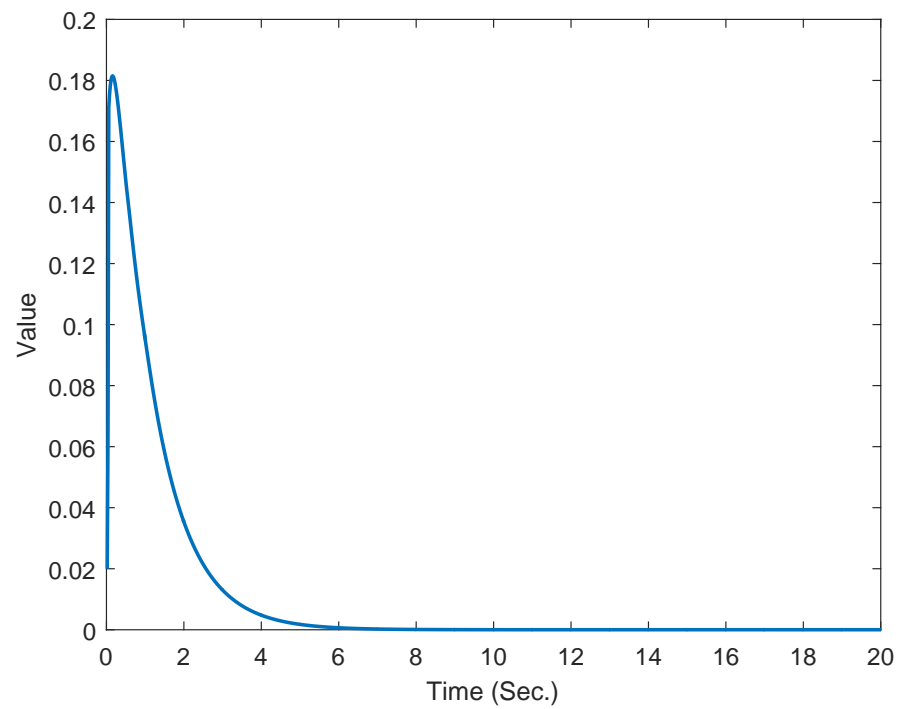


Figure 8. The trajectory of $\hat{\chi}$ for case 2.

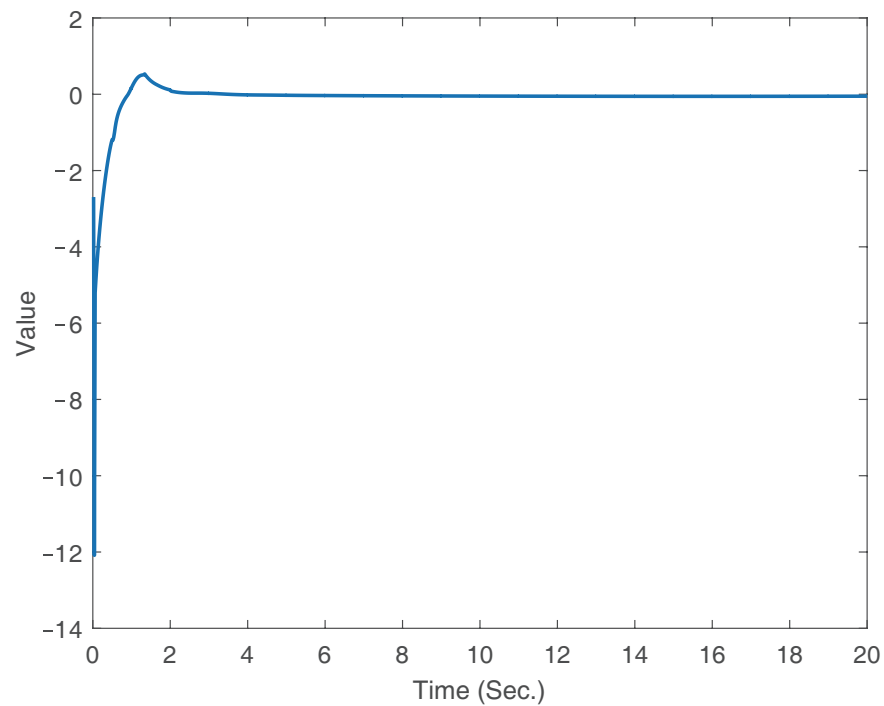


Figure 9. The trajectory of state x_2 for case 2.

To make a more equal comparison, the same parameters were designed for the finite-time controller and our proposed fixed-time controller. The simulation results using a finite-time controller and our proposed fixed-time controller are given in Figures 10 and 11.

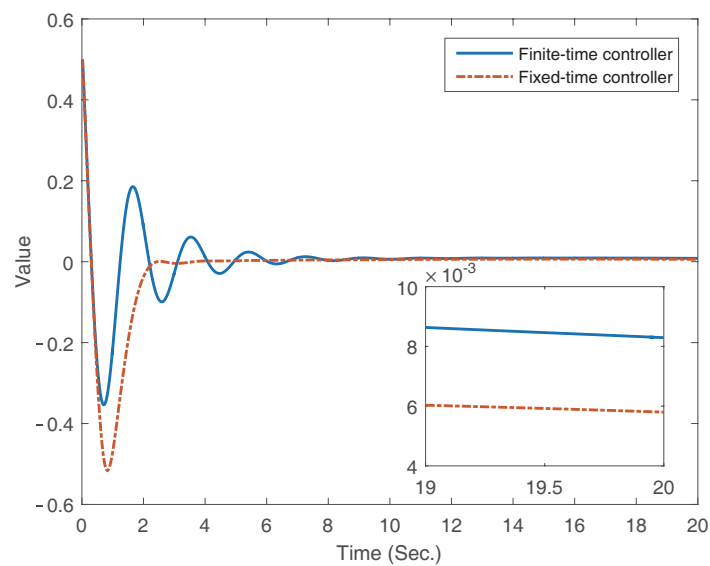


Figure 10. The trajectory of state x_1 for case 1.

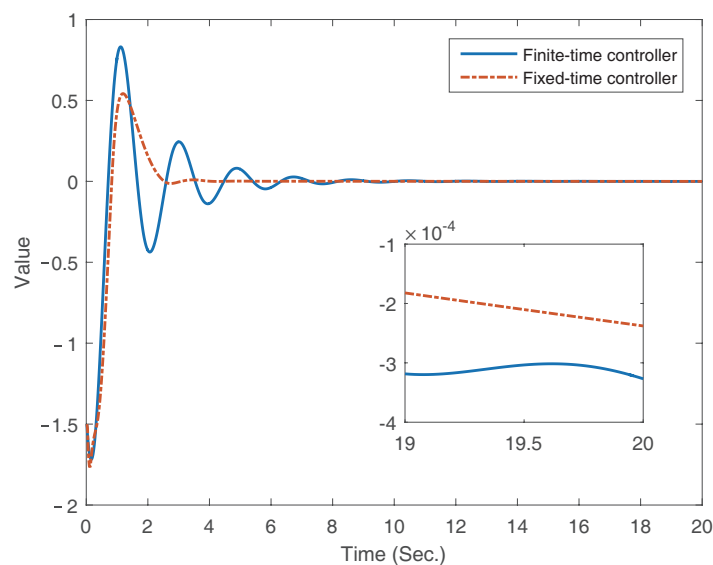


Figure 11. The trajectory of state x_2 for case 1.

From Figure 10, it can be observed that, with the finite-time controller and fixed-time controller, system state x_1 converges to near-zero within 4 s and 10 s, respectively. By 20 s, the control precision is approximately 8×10^{-3} for the finite-time controller and 5.8×10^{-3} for the fixed-time controller. From Figure 11, it can be observed that, with the finite-time controller and fixed-time controller, system state x_2 converges to near-zero within 4 s and 10 s, respectively. By 20 s, the control precision is approximately 3.2×10^{-3} for the finite-time controller and 1.5×10^{-3} for the fixed-time controller. From the comparative simulation results, it is evident that, in the absence of a disturbance observer, the perturbations in the trajectories of states x_1 and x_2 are significantly enhanced, and their control precision is also lower compared to the scenario where a disturbance observer is present. Additionally, it can be observed that the convergence speed of the fixed-time controller is faster than that of the finite-time controller. Based on the simulation results, we can deduce that our derived control protocol guarantees rapid convergence performance for the closed-loop system. Moreover, the two cases' simulation results

confirm that the derived adaptive fixed-time fuzzy controller in this work can effectively mitigate the impact of mismatched disturbances.

5. Conclusions

This paper addressed the fixed-time fuzzy control issue for uncertain nonlinear systems with mismatched disturbances. The systems encompass mismatched disturbances and unknown nonlinear functions. Through the utilization of the adaptive method and disturbance observers, a range of issues stemming from uncertain nonlinear functions and mismatched disturbances have been effectively addressed. By applying the backstepping technique and incorporating the concept of integrating one power integrator, we have developed a fixed-time fuzzy adaptive control protocol for uncertain nonlinear systems. This controller design guarantees the fixed-time stability of the controlled systems. A practical example has been showcased to illustrate the efficacy of the derived controller. Future investigations will involve extending our proposed control approach to uncertain systems featuring full-state constraints.

Author Contributions: R.L.: software, conceptualization, methodology, writing, and investigation. L.Z.: writing, conceptualization, methodology, and investigation. Y.L.: methodology, investigation, and writing. All authors have read and agreed to the published version of the manuscript.

Funding: This research received no external funding.

Data Availability Statement: Data are contained within the article.

Conflicts of Interest: The authors declare no conflicts of interest.

References

1. Yang, C.; Jiang, Y.; Na, J.; Li, Z.; Cheng, L.; Su, C. Finite-time convergence adaptive fuzzy control for dual-arm robot with unknown kinematics and dynamics. *IEEE Trans. Fuzzy Syst.* **2018**, *27*, 574–588. [\[CrossRef\]](#)
2. Sun, K.; Karimi, H.R.; Qiu, J. Finite-time fuzzy adaptive quantized output feedback control of triangular structural systems. *Inf. Sci.* **2021**, *557*, 153–169. [\[CrossRef\]](#)
3. Lv, X.; Niu, Y.; Song, J. Finite-time boundedness of uncertain Hamiltonian systems via sliding mode control approach. *Nonlinear Dyn.* **2021**, *104*, 497–507. [\[CrossRef\]](#)
4. Ye, D.; Sun, J.; Xiao, Y.; Sun, Z. Energy optimal guidance for proximity approach with obstacle avoidance. *Aerosp. Sci. Technol.* **2022**, *130*, 107949. [\[CrossRef\]](#)
5. Yu, J.; Shi, P.; Chen, X.; Cui, G. Finite-time command filtered adaptive control for nonlinear systems via immersion and invariance. *Sci. China Inf. Sci.* **2021**, *64*, 192202. [\[CrossRef\]](#)
6. Wang, A.; Liu, L.; Qiu, J.; Feng, G. Finite-time adaptive fuzzy control for nonstrict-feedback nonlinear systems via an event-triggered strategy. *IEEE Trans. Fuzzy Syst.* **2019**, *28*, 2164–2174. [\[CrossRef\]](#)
7. Mehdifar, F.; Hashemzadeh, F.; Baradarannia, M.; de Queiroz, M. Finite-time rigidity-based formation maneuvering of multiagent systems using distributed finite-time velocity estimators. *IEEE Trans. Cybern.* **2018**, *49*, 4473–4484. [\[CrossRef\]](#) [\[PubMed\]](#)
8. Witkowska, A.; Tomera, M.; Śmierczalski, R. A backstepping approach to ship course control. *Int. J. Appl. Math. Comput. Sci.* **2007**, *17*, 73–85. [\[CrossRef\]](#)
9. Li, G.; Wang, X.; Li, S. Consensus control of higher-order Lipschitz non-linear multi-agent systems based on backstepping method. *IET Control. Theory Appl.* **2019**, *14*, 490–498. [\[CrossRef\]](#)
10. Kartal, Y.; Subbarao, K.; Gans, N.R.; Dogan, A.; Lewis, F. Distributed backstepping based control of multiple UAV formation flight subject to time delays. *IET Control. Theory Appl.* **2020**, *14*, 1628–1638. [\[CrossRef\]](#)
11. Zhuang, H.; Sun, Q.; Chen, Z.; Zeng, X. Robust adaptive sliding mode attitude control for aircraft systems based on back-stepping method. *Aerosp. Sci. Technol.* **2021**, *118*, 107069. [\[CrossRef\]](#)
12. Zhang, L.; Ding, H.; Shi, J.; Huang, Y.; Chen, H.; Guo, K.; Li, Q. An adaptive backstepping sliding mode controller to improve vehicle maneuverability and stability via torque vectoring control. *IEEE Trans. Veh. Technol.* **2020**, *69*, 2598–2612. [\[CrossRef\]](#)
13. Xiao, Y.; de Ruiter, A.; Ye, D.; Sun, Z. Attitude coordination control for flexible spacecraft formation flying with guaranteed performance bounds. *IEEE Trans. Aerosp. Electron. Syst.* **2022**, *59*, 1534–1550. [\[CrossRef\]](#)
14. Yu, J.; Shi, P.; Zhao, L. Finite-time command filtered backstepping control for a class of nonlinear systems. *Automatica* **2018**, *92*, 173–180. [\[CrossRef\]](#)
15. Capone, A.; Hirche, S. Backstepping for partially unknown nonlinear systems using Gaussian processes. *IEEE Control Syst. Lett.* **2019**, *3*, 416–421. [\[CrossRef\]](#)

16. Fedele, G.; Dlfonso, L. A kinematic model for swarm finite-time trajectory tracking. *IEEE Trans. Cybern.* **2018**, *49*, 3806–3815. [[CrossRef](#)]
17. Wang, H.; Yu, W.; Ren, W.; Lu, J. Distributed adaptive finite-time consensus for second-order multiagent systems with mismatched disturbances under directed networks. *IEEE Trans. Cybern.* **2019**, *51*, 1347–1358. [[CrossRef](#)] [[PubMed](#)]
18. Xiao, W.; Ren, H.; Zhou, Q.; Li, H.; Lu, R. Distributed finite-time containment control for nonlinear multiagent systems With mismatched disturbances. *IEEE Trans. Cybern.* **2022**, *52*, 6939–6948. [[CrossRef](#)]
19. Wang, H.; Yu, W.; Ren, W.; Lu, J. Finite-time output consensus of higher-order multi-agent systems with mismatched disturbances and unknown state elements. *IEEE Trans. Syst. Man Cybern. Syst.* **2019**, *66*, 2571–2581.
20. Arabi, E.; Yucelen, T.; Singler, J.R. Finite-time distributed control with time transformation. *Int. J. Robust Nonlinear Control.* **2021**, *31*, 107–130. [[CrossRef](#)]
21. Yu, J.; Shi, P.; Liu, J.; Lin, C. Neuroadaptive finite-time control for nonlinear MIMO systems with input constraint. *IEEE Trans. Cybern.* **2020**, *52*, 6676–6683. [[CrossRef](#)] [[PubMed](#)]
22. Ye, D.; Zou, A.; Sun, Z. Predefined-time predefined-bounded attitude tracking control for rigid spacecraft. *IEEE Trans. Aerosp. Electron. Syst.* **2022**, *58*, 464–472. [[CrossRef](#)]
23. Zhao, L.; Yu, J.; Chen, X. Neural-network-based adaptive finite-time output feedback control for spacecraft attitude tracking. *IEEE Trans. Neural Netw. Learn. Syst.* **2023**, *34*, 8116–8123. [[CrossRef](#)] [[PubMed](#)]
24. Fang, L.; Wu, C.; Ji, H. Distributed adaptive finite-time consensus for high-order multi-agent systems with intermittent communications under switching topologies. *Symmetry* **2022**, *14*, 1368. [[CrossRef](#)]
25. Mouktonglang, T.; Poochinapan, K.; Yimnet, S. Robust finite-time control of discrete-time switched positive time-varying delay systems with exogenous disturbance and their application. *Symmetry* **2022**, *14*, 735. [[CrossRef](#)]
26. Alattas, K.A.; Mobayen, S.; Assawinchaichote, W.; Asad, J.H.; Awrejcewicz, J.; Aly, A.A.; Alghtani, A.H. The remaining authors are added, please check and confirm. We confirm that no problem. A Lyapunov-based optimal integral finite-time tracking control approach for asymmetric nonholonomic robotic systems. *Symmetry* **2021**, *13*, 2367. [[CrossRef](#)]
27. Mei, K.; Ding, S. Fixed-time HOSM controller design for constrained sliding mode systems with mismatched terms. *Inf. Sci.* **2022**, *585*, 366–381. [[CrossRef](#)]
28. Cai, Y.; Zhang, H.; Zhang, J.; Wang, W. Fixed-time leader-following/containment consensus for a class of nonlinear multi-agent systems. *Inf. Sci.* **2021**, *555*, 58–84.
29. Li, Q.; Wei, J.; Gou, Q.; Niu, Z. Distributed adaptive fixed-time formation control for second-order multi-agent systems with collision avoidance. *Inf. Sci.* **2021**, *564*, 27–44. [[CrossRef](#)]
30. Sun, Y.; Wang, F.; Liu, Z.; Zhang, Y.; Chen, C.P. Fixed-time fuzzy control for a class of nonlinear systems. *IEEE Trans. Cybern.* **2020**, *52*, 3880–3887. [[CrossRef](#)]
31. Jiang, B.; Li, C.; Hou, S.; Ma, G. Fixed-time attitude tracking control for spacecraft based on adding power integrator technique. *Int. J. Robust Nonlinear Control* **2020**, *30*, 2515–2532. [[CrossRef](#)]
32. Ba, D.; Li, Y.; Tong, S. Fixed-time adaptive neural tracking control for a class of uncertain nonstrict nonlinear systems. *Neurocomputing* **2019**, *363*, 273–280. [[CrossRef](#)]
33. Li, K.; Hua, C.; You, X.; Guan, X. Finite-time observer-based leader-following consensus for nonlinear multiagent systems with input delays. *IEEE Trans. Cybern.* **2020**, *51*, 5850–5858. [[CrossRef](#)] [[PubMed](#)]
34. Chen, M.; Wang, H.; Liu, X. Adaptive fuzzy practical fixed-time tracking control of nonlinear systems. *IEEE Trans. Fuzzy Syst.* **2019**, *29*, 664–673. [[CrossRef](#)]
35. Han, H.; Liu, H.; Li, J.; Qiao, J. Cooperative fuzzy-neural control for wastewater treatment process. *IEEE Trans. Ind. Inform.* **2020**, *17*, 5971–5981. [[CrossRef](#)]
36. Liu, R.; Liu, M.; Ye, D.; Yu, Y. Event-triggered adaptive fixed-time fuzzy control for uncertain nonlinear systems with unknown actuator faults. *Inf. Sci.* **2022**, *612*, 344–360. [[CrossRef](#)]
37. Sun, H.; Hou, L.; Zong, G.; Yu, X. Fixed-time attitude tracking control for spacecraft with input quantization. *IEEE Trans. Aerosp. Electron. Syst.* **2018**, *55*, 124–134. [[CrossRef](#)]
38. Zhao, L.; Yu, J.; Lin, C.; Yu, H. Distributed adaptive fixed-time consensus tracking for second-order multi-agent systems using modified terminal sliding mode. *Appl. Math. Comput.* **2017**, *312*, 23–35. [[CrossRef](#)]
39. Qian, C.; Lin, W. A continuous feedback approach to global strong stabilization of nonlinear systems. *IEEE Trans. Autom. Control.* **2001**, *46*, 1061–1079. [[CrossRef](#)]
40. Zou, A.; Kumar, K.D.; de Ruiter, A.H. Fixed-time attitude tracking control for rigid spacecraft. *Automatica* **2020**, *113*, 108792. [[CrossRef](#)]
41. Liu, J.; Zhang, Y.; Yu, Y.; Sun, C. Fixed-time event-triggered consensus for nonlinear multiagent systems without continuous communications. *IEEE Trans. Syst. Man Cybern. Syst.* **2018**, *49*, 2221–2229. [[CrossRef](#)]
42. Yu, W.; Ren, W.; Zheng, W.X.; Chen, G.; Lü, J. Distributed control gains design for consensus in multi-agent systems with second-order nonlinear dynamics. *Automatica* **2013**, *49*, 2107–2115. [[CrossRef](#)]
43. Xu, H.; Yu, D.; Sui, S.; Zhao, Y.; Chen, C.P.; Wang, Z. Nonsingular practical fixed-time adaptive output feedback control of MIMO nonlinear systems. *IEEE Trans. Neural Netw. Learn. Syst.* **2022**, *34*, 7222–7234. [[CrossRef](#)] [[PubMed](#)]

-
44. Liu, Y.; Jiang, B.; Lu, J.; Cao, J.; Lu, G. Event-triggered sliding mode control for attitude stabilization of a rigid spacecraft. *IEEE Trans. Syst. Man Cybern. Syst.* **2018**, *50*, 3290–3299. [[CrossRef](#)]
 45. Wu, B.; Shen, Q.; Cao, X. Event-triggered attitude control of spacecraft. *Adv. Space Res.* **2018**, *61*, 927–934. [[CrossRef](#)]

Disclaimer/Publisher’s Note: The statements, opinions and data contained in all publications are solely those of the individual author(s) and contributor(s) and not of MDPI and/or the editor(s). MDPI and/or the editor(s) disclaim responsibility for any injury to people or property resulting from any ideas, methods, instructions or products referred to in the content.